Diffraction from oxide confinement apertures in vertical-cavity lasers

P. A. Roos and J. L. Carlsten[a)]
Montana State University, Department of Physics, Bozeman, Montana 59717

D. C. Kilper
University of North Carolina at Charlotte, Department of Physics, Charlotte, North Carolina 28223

K. L. Lear
MicroOptical Devices Inc., 5601C Midway Park Pl. NE, Albuquerque, New Mexico 87109

(Received 22 February 1999; accepted for publication 12 June 1999)

Direct measurement of scattered fields from oxide confinement apertures in vertical-cavity lasers is presented. Diffraction fringes associated with each transverse lasing mode are detected in the far field from devices with varying oxide aperture dimensions and with quantum efficiencies as high as 48%. The diffracted pattern symmetries match the rectangular symmetry of the oxide apertures present in the devices and fringe locations are compared to Fraunhofer theory. The fraction of power diffracted from the lasing mode remains roughly constant as a function of relative pump rate, but is shown to depend on both transverse mode order and oxide aperture size. © *1999 American Institute of Physics.* [S0003-6951(99)03532-9]

Selective oxidation as a means of electrical and optical confinement has dramatically enhanced the performance of vertical-cavity surface-emitting lasers (VCSELs). The benefits of oxide confinement are manifest in properties ranging from low laser threshold[1] and decreased intensity noise[2] to high differential quantum efficiencies and increased modulation bandwidth[3] as compared to other confinement methods such as proton implantation. By growing the laterally confining oxide aperture dimensions smaller and thereby increasing optical losses to higher order transverse modes, single fundamental mode laser operation has also been achieved.[4]

But such lateral confinement is not without cost. Due to the abrupt nature of the index step between the oxide cladding region and the unoxidized optical cavity,[4] there can exist a phase discontinuity in the field at this boundary. Scattering losses due to such discontinuities are predicted to increase with decreasing aperture dimensions.[5] Since aperture dimensions on the order of several wavelengths are necessary to obtain single transverse mode operation, a delicate balance ensues between the desired optical confinement and the unwanted scattering from the confinement boundary. Such scattering losses have been shown to play a critical role in laser performance,[5,6] but have not been directly measured. In this letter, we present direct observation of diffraction patterns from oxide confinement boundaries and we measure diffracted field intensities relative to the undiffracted lasing mode.

The devices used in this experiment consist of AlGaAs laser cavities grown to match a nominal lasing wavelength of 960 nm. Distributed Bragg reflectors serve as the top (output) and bottom mirrors with reflectivities of $>99.0\%$ and $>99.9\%$, respectively. The laser cavities are sandwiched between two oxide confinement layers with square or rectangular apertures varying between $\sim 4.5\ \mu m \times 4.5\ \mu m$ and $\sim 12\ \mu m \times 12\ \mu m$ (see Ref. 3 for similar device construction). Smaller device apertures were not available for investigation. The oxide layers are of a quarter wave thickness and are positioned on the first low index layer. The active regions are three 8 nm InGaAs quantum wells. Although each device operates in a single longitudinal mode, the number of transverse lasing modes typically varies between one and six, depending on the drive current.

With traditional methods of beam profiling it is difficult to extract the individual transverse mode profiles for these devices due to the spatial overlap of the modes. However, since each transverse mode has a distinct cavity resonance, following previous work,[7] we utilize the frequency separation of these modes as a discriminator. As depicted in Fig. 1, a multimode optical fiber is scanned along the curved wavefront of the uncollimated VCSELs in the far field. The source-to-fiber distance is 2.4 cm for all data taken. Optical feedback was avoided and associated effects were not observed. At each angular position of the fiber, the signal is spectrally resolved using a spectrometer. In this manner, the optical power of each transverse mode can be monitored as a function of azimuthal and polar angles. If the spectrometer output is logarithmically amplified, this method can provide more than five orders of magnitude in dynamic range. All results were highly reproducible even when the laser was rotated or translated slightly from its original position indicating that coupling into and transmission through the fiber was not greatly affected by polarization or precise alignment.

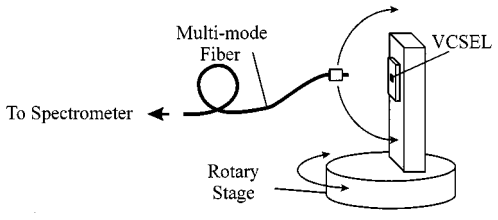

FIG. 1. Light collection apparatus. Light from the fiber is spectrally analyzed using a spectrometer.

[a)]Electronic mail: carlsten@physics.montana.edu

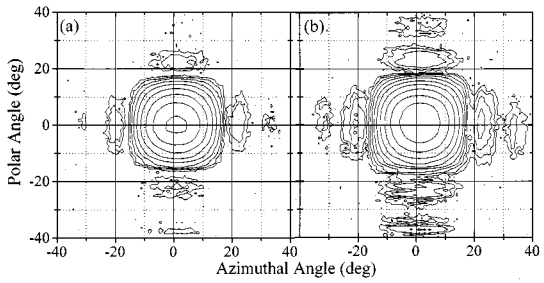

FIG. 2. Detected optical power vs polar and azimuthal angles for the fundamental (0,0) transverse mode. Relative pump rates $(I-I_{th})/I_{th}$ of (a) 1.76 and (b) 17.8 are shown. The lowest contour represents −96 dBm and the highest represents −53 dBm resulting in a 4.3 dBm contour spacing. This data indicates that fringe position is independent of relative pump rate. Two-dimensional integration over the mode profiles showed that fractional diffracted power remained constant for the two relative pump rates.

Figure 2 shows two-dimensional logarithmic intensity profiles of the fundamental transverse mode for a device with ~4.5 μm×4.5 μm aperture, operating at relative pump rates $(I-I_{th})/I_{th}$ of (a) 1.76 and (b) 17.8. Note that the plot axes are the two angles of spherical polar coordinates and that representation on a flat, square plane necessarily causes some distortion. Interference maxima and minima are clearly observed in both plots. Although the absolute diffracted power of the device scales roughly with relative pump rate, the fractional diffracted power $[(4.4\pm0.2)\times10^{-3}$ for this device] and the locations of the interference minima did not measurably depend on pump rate. Fractional diffracted power was determined by taking the ratio of the integrated diffracted optical power to that contained in the undiffracted mode. Note, however, that this fractional power does not include the losses due to additional reflections in the VCSEL mesa structure, nor does it include losses due to the back aperture in the cavity. The observed radiation pattern was common to all devices studied and matches the expected pattern for the rectangular oxide apertures present in these devices.

Fraunhofer theory was used to verify the diffraction source. On a logarithmic scale, Fig. 3 shows data (squares) for a single slice through the center of the fundamental mode profile of the same device at zero polar angle, operating at a relative pump rate of 17.8. A simple calculation of the far-field diffraction pattern due to a Gaussian beam profile within the cavity, truncated by an opaque aperture, gives good agreement with the features present in the experimental data. The dashed curve in Fig. 3 shows the resulting intensity profile calculated for a *1/e* field diameter of 4.19 μm and an aperture size of 4.53 μm, in good agreement with the expected values. The calculation assumes a field amplitude maximum centered within the aperture and refraction due to the laser medium/air interface was included. Discrepancies in the diffracted maxima amplitudes can be attributed to our use of an opaque aperture as compared to the index step present in the actual device. Also, attenuation of the field at higher angles is expected due to the distributed Bragg reflectors as well as the laser medium/air interface and the gain of the laser. A slight asymmetry was observed in the diffraction pattern of some device profiles, indicating that either the peak of the field amplitude is not centered in the aperture or the propagation vector of the outgoing field is not perpendicular to the plane of the aperture. This effect may occur for example if the oxide apertures on the top and bottom sides of the cavity were slightly misaligned with respect to each other. We also note that diffraction is observed here despite the high differential quantum efficiency (up to 48%) of some devices. Therefore, the diffraction is observable even in high efficiency devices with presumably low scattering losses.

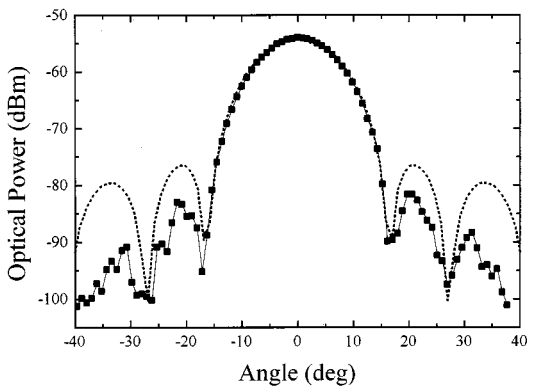

FIG. 3. Optical power vs azimuthal angle. The polar angle was held at zero degrees. The fundamental (0,0) mode is shown on a log scale (squares) for a relative pump rate $(I-I_{th})/I_{th}$ of 17.8. The dotted curve represents a Fraunhofer diffraction of a Gaussian beam truncated by an opaque slit.

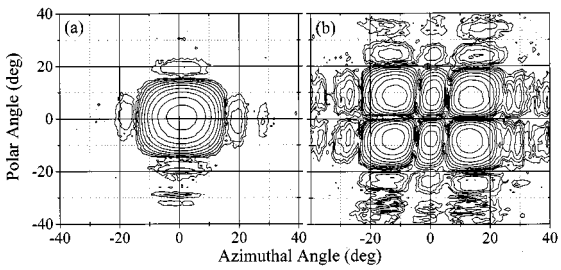

FIG. 4. Detected optical power vs polar and azimuthal angles for (a) the fundamental (0,0) mode and (b) the (2,1) higher order transverse mode of a ~6 μm×6 μm aperture device. The lowest contour represents −96 dBm and the highest represents −55 dBm resulting in a 4 dBm contour spacing. Integration over the profiles showed that fractional diffracted power was larger for the higher order mode.

Figure 4 shows logarithmic intensity profiles for (a) the (0,0) fundamental and (b) the (2,1) higher order transverse modes for a device with ~6 μm×6 μm aperture. A drive

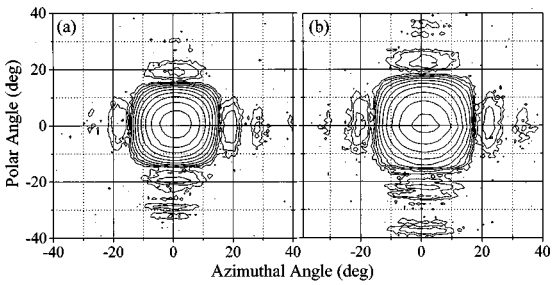

FIG. 5. Detected optical power of the (0,0) mode vs polar and azimuthal angles for (a) a ~4.5 μm×4.5 μm and (b) a ~6 μm×6 μm aperture device. The lowest contour represents −96 dBm and the highest represents −55 dBm resulting in a 4.1 dBm contour spacing. This plot indicates that the diffracted maxima positions move to larger angles for smaller aperture sizes. Integration over the profiles showed that fractional diffracted power increases for smaller aperture sizes.

current was chosen such that the total optical power was roughly the same for the two modes. As expected, diffraction from the oxide layers is not restricted to the fundamental mode. Furthermore, the higher order transverse mode diffracts a larger fraction of its power $[(8.5\pm0.5)\times10^{-3}]$ as compared to the fundamental mode $[(3.7\pm0.2)\times10^{-3}]$. This observation qualitatively matches theoretical predictions, and is expected considering the higher order modes have more power concentrated near the aperture boundary.

Figure 5 shows logarithmic intensity profiles of the fundamental transverse mode for devices with (a) $\sim$4.5 μm $\times$4.5 μm and (b) $\sim$6 μm$\times$6 μm apertures. Pump rates for each device were chosen such that the optical power was roughly equal for the two plots. As expected, the diffraction maxima positions move to larger angles with decreasing aperture size. Furthermore, fractional diffracted power was measured to increase with decreasing aperture size from $(3.7\pm0.2)\times10^{-3}$ to $(4.4\pm0.2)\times10^{-3}$, representing an increase of $19\pm4\%$. Uncertainty in these values resulted from uncertain first order minima positions used for integration. Optical losses from the fundamental mode due to such diffraction can therefore play a role in determining the minimum aperture dimensions allowable for laser operation.

This work was supported by the NSF–EPSCOR, NASA–EPSCOR, ILX Lightwave, and the DOE.

[1] K. D. Choquette, K. L. Lear, R. P. Schneider, Jr., and K. M. Geib, Appl. Phys. Lett. **66**, 3413 (1995).
[2] D. C. Kilper, P. A. Roos, J. L. Carlsten, and K. L. Lear, Phys. Rev. A **55**, R3323 (1997).
[3] K. L. Lear, A. Mar, K. D. Choquette, S. P. Kilcoyne, R. P. Schneider, Jr., and K. M. Geib, Electron. Lett. **31**, 208 (1995).
[4] K. L. Lear, K. D. Choquette, R. P. Schneider, Jr., and S. P. Kilcoyne, Appl. Phys. Lett. **66**, 2616 (1995).
[5] E. R. Hegblom, D. I. Babic, B. J. Thibeault, and L. A. Coldren, Appl. Phys. Lett. **68**, 1757 (1996).
[6] K. L. Lear, S. P. Kilcoyne, and S. A. Chalmers, IEEE Photonics Technol. Lett. **6**, 778 (1994).
[7] C. J. Chang-Hasnain, J. P. Harbison, and G. Hasnain, IEEE J. Quantum Electron. **27**, 1402 (1991).